THE ASTROPHYSICAL JOURNAL, 414:463–473, 1993 September 10

THE PLANETARY NEBULA SYSTEM AND DYNAMICS OF NGC 5128. I. PLANETARY NEBULAE AS STANDARD CANDLES

XIAOHUI HUI,[1,2,3,4,5] HOLLAND C. FORD,[2,5,6] ROBIN CIARDULLO,[5,7,8] AND GEORGE H. JACOBY[5,9]
Received 1992 Ocotober 6; accepted 1993 March 19

ABSTRACT

We present the result of a planetary nebula (PN) survey of the nearby giant elliptical galaxy NGC 5128 performed with CCD cameras at the prime focus of the CTIO 4 m telescope. By comparing CCD images centered on the characteristic emission line [O III] λ5007 and on the adjacent continuum, we identify a total of 785 PNs in areas extending 20 kpc along the photometric major axis and covering the whole galaxy to 10 kpc. From these data, we form a complete sample of 224 PNs extending to a dereddened limiting magnitude of $m_{5007} = 24.8$, which extends 1.5 mag down the PN luminosity function (PNLF). Adopting a foreground extinction of $E(B-V) = 0.1$, we derive a distance to the galaxy of 3.5 ± 0.2 Mpc, in excellent agreement with the surface brightness fluctuation method. No population effect on the bright cutoff of PNLF is observed in the isophotal radius range of 2–16 kpc, but the luminosity specific PN density ($\alpha_{2.5}$) seems to increase with radius inside of 7 kpc, in agreement with the $\alpha_{2.5}$-color relation observed for other galaxies.

Subject headings: distance scale — galaxies: individual (NGC 5128) — planetary nebulae: general

1. INTRODUCTION

The study of extragalactic planetary nebulae (PNs) has made rapid progress in recent years with the help of high quantum efficiency detectors. A brief but distinctive phase in the late stage of stellar evolution, PNs are not only interesting objects in their own right, but also extremely valuable and unique tools for probing their host galaxies. Among the focuses of recent studies are (1) the use of PNs as test particles to study the dynamics and mass distributions in galactic halos, (2) the use of PNs to probe galactic chemical evolution, and (3) the use of the PN luminosity function as a standard candle to measure extragalactic distances. It is this latter use that is the main topic of this paper.

PNs are among the best standard candles for extragalactic distance measurements. Ford & Jenner (1978) and Jacoby & Lesser (1981) first noticed that the brightest PNs in M31 and in several Local Group dwarf ellipticals have a similar brightness. Ciardullo et al. (1989a) further studied the top 2.5 mag of the PNLF in the bulge of M31 and found that, while the faint end of the PNLF follows the exponential distribution expected for uniformly expanding nebula shells, at bright magnitudes the function is truncated rather abruptly. As demonstrated by the recent PNLF studies of the Magellanic Clouds (Jacoby, Walker, & Ciardullo 1990b), M81 (Jacoby et al. 1989), the Leo I Group (Ciardullo, Jacoby & Ford 1989b), the NGC 1023 Group (Ciardullo, Jacoby, & Harris 1991), and the Virgo Cluster (Jacoby, Ciardullo, & Ford 1990a), this cutoff is an excellent standard candle.

The internal consistency of the PNLF distances has been thoroughly tested by observing galaxies within common groups and clusters. No significant systematic effect has been observed in the Leo I Group (three galaxies) or the Virgo Cluster (six galaxies), despite the fact that the central metallicity of these galaxies varies between $0.15 \leq [\mathrm{Fe/H}] \leq 0.41$ (Ciardullo et al. 1991). The reliability of the method has been further demonstrated by comparing PNLF distances with distances derived from other standard candles. The PNLF distances to the Magellanic Clouds and M81 are in excellent agreement with that derived from the *I*-band and infrared observations of Cepheids. Moreover, the dispersion between the PNLF distance and distances derived for 14 galaxies with the surface brightness fluctuation method is only 0.17 mag (Jacoby et al. 1992).

Nevertheless, fewer than 25 galaxies have been the subject of a PN survey, and no galaxy outside the Local Group has had both a deep and comprehensive survey made of its PN population. As a result, the internal PNLF tests have always involved the intercomparison of PN samples from different galaxies and have usually been restricted to less than 100 objects. In order to investigate the behavior of the PNLF within a single galaxy, a deep PN survey is needed in a large, nearby galaxy.

Here we present the results of a PN survey of NGC 5128 (also known as radio source Centaurus A), a giant elliptical galaxy with a prominent dust lane lying along its photometric minor axis. In this survey we identify a total of 785 PNs in a region extending 20 kpc along the photometric major axis and covering the entire central 10 kpc of the galaxy. We will publish the survey results in two parts. In this paper we describe the PN survey, form the PN luminosity function, and derive the galaxy's PNLF distance. The large sample size and the extensive spatial coverage of the data allow a unique opportunity to study any radial variation of the PN luminosity function. Because the PN catalog is quite lengthy, it will appear in a second paper in the *Astrophysical Journal Supple-*

[1] Astronomy Department, Boston University, Boston, MA 02215.
[2] Physics and Astronomy Department, the Johns Hopkins University, Baltimore, MD 21218.
[3] Hubble Fellow.
[4] Astronomy Department, California Institute of Technology, Pasadena, CA 91125.
[5] Visiting astronomer, Cerro Tololo Inter-American Observatory, operated by the Association of Universities for Research in Astronomy, Inc., under contract with the National Science Foundation.
[6] Space Telescope Science Institute, Baltimore, MD 21218.
[7] Astronomy Department, Penn State University, University Park, PA 16802.
[8] 1992 NSF Young Investigator.
[9] Kitt Peak National Observatory, NOAO, Tucson, AZ 85726.

ment (Hui et al. 1993a, hereafter Paper II). In a third paper (Hui et al. 1993b, hereafter Paper III), we will present accurate velocities for over 400 of these PNs and discuss the dynamics and mass distribution of the galaxy.

The paper is arranged as follows. In the first sections we describe the observations and CCD data reductions (§ 2), the PN flux calibrations (§ 3), and the positional measurements (§ 4). Section 5 presents the spatial distribution of NGC 5128 PNs; it also directs the readers to Paper II which presents a catalog of the PNs along with tables of bright astrometric reference stars. We follow this data presentation by analyzing the completeness of the PNLF, deriving the distance to the galaxy (§ 6), examining the variation of the PNLF with galactic radius, and comparing the survey results to observations of other galaxies (§ 7 and § 8). Finally, a short summary is given in § 9.

2. OBSERVATIONS AND REDUCTIONS

2.1. *Observations*

Our PN observations of NGC 5128 took place over three observing seasons. During 1985 and 1986, we took [O III] λ5007 on-band/off-band pictures of selected galaxy fields using the RCA CCD camera at the prime focus of the CTIO 4 m telescope. In 1988 a third survey was carried out on the same telescope with a TI CCD. The instrument setups for the three surveys are listed in Table 1, and a journal of the observations is given in Table 2. The typical exposure times were 1 hr for an on-band image and 575 s for an off-band frame. The latter was exposed intentionally 0.25 mag deeper so that the higher signal-to-noise ratio in the off-band would prevent spurious identifications near the frame limit. At the beginning and the end of each night, we also observed two or three photometric standard stars for the PN flux calibration. The observed standards were EG 54, EG 63, EG 274, LTT 6248, LTT 7379, and BD +8°2015 (Stone & Baldwin 1983; Stone 1977; Oke 1974).

Because the CCDs were much smaller than the full extent of the galaxy, we placed our survey fields where the PN velocities are most crucial for understanding the kinematical properties of the galaxy. The rectangular RCA CCD fields in Figure 1 (Plate 4) were chosen along the photometric major axis of NGC 5128's faint outer isophotes (Dufour et al. 1979, hereafter D79) and on both sides of the galaxy in order to measure rotation in the halo. Adopting 305″ as the effective radius, r_e, these fields are between 2 and $4r_e$ from the galaxy's center. The radial distances of the halo fields were a compromise between observing as far as possible into the halo and the low detection rate in fields more distant than the outermost one shown in Figure 1. The square TI CCD fields in the figure, which are observed in the third run, were positioned both to study the minor axis rotation of the galaxy and to fill in the gaps between the two central fields and major axis halos fields.

TABLE 1

PN SURVEY ON THE PF OF THE CTIO 4 m TELESCOPE

PARAMETER	DATE		
	1985 March	1986 April	1988 April
CCD detector	RCA	RCA	TI
e^-/ADU	~10.5	~9	~1.4
Readout noise (e^-)	~80	~80	~5.5
QE (5000 Å)	~40%	~40%	~60%
Format	300 × 508	300 × 508	800 × 800
Pixel size	30 μm, 0.″56	30 μm, 0.″56	15 μm, 0.″28
Number of fields	7	20	16
λ_c/FWHM (Å)[a]	5019/27	5017/27	5017/37
T_{λ_c}[b]	63.5%	63.5%	66.5%

[a] In an f/2.77 beam and at the dome temperature of 12.°8 C for the 1985 and 1986 runs and 14° C for the 1988 run.

[b] Filter transmission at λ_c.

2.2. *Identifications*

Basic CCD reductions such as bias subtraction and flat-fielding were made during the observing run. To identify PNs, we scaled our on-band/off-band images to the same apparent brightness and blinked the two frames on an image display. Our identification criteria for planetary nebulae were (1) appearance in the on-band frame, (2) absence in the off-band frame, and (3) a point profile. In total, 785 planetary nebulae were identified on the 43 CCD fields.

In general, the three criteria listed above are sufficient to identify PNs in elliptical galaxies. However, NGC 5128 is known for having an abundance of discrete H II regions along its dust lane (Graham 1979). We therefore used Ciardullo et al.'s (1990) Hα images of the two central fields (fields 2 and 5) to exclude from our PN sample those low excitation objects with Hα brighter than [O III] λ5007.

In other fields near the dust lane, we excluded those emission-line objects which were resolved. In addition, because the kinematical properties of the dust lane are distinctively different from those of the elliptical component, we were able to further eliminate candidates whose velocities were characteristic of the dust lane (Paper III). In total, 17 PN candidates were reclassified as H II regions, with most of them satisfying both criteria. The presence of a strong Hβ line in those objects observed in our spectroscopic program (Paper III) later confirmed their nature as H II regions.

2.3. *CCD Reductions*

Photometric reductions were performed using the FORTRAN version of the DAOPHOT package (Stetson 1987). In each [O III] λ5007 frame, several isolated bright stars were carefully selected on an image display. A point-spread function (PSF) was then constructed from these stars. Because PNs are mostly isolated objects in the CCD frames, the DAOPHOT routine PEAK, which fits the PSF to individual stars, was run to derive their instrumental magnitudes and (x, y) positions.

For the 1985 and 1986 data, the DAOPHOT parameter *fitting radius* was set to 2 pixels, a value which corresponds to an average seeing 1.″2. Only pixels within this radius were used in the PSF fitting. The sky background level was then measured in an annulus between 12 and 25 pixels around each nebula. This simple procedure produced satisfactory results for measurements in 25 of our 27 fields. However, for the two central fields (fields 2 and 5), the rapidly changing background of the galaxy affected the measurements of the local sky, and thereby reduced the photometric accuracy. To improve the photometry on these frames, we registered, scaled, and subtracted our off-band images from our on-band frames, to produce a "difference" frame. This procedure effectively flattened the sky background and improved the photometry. Because the photometric error in even the brightest PN was dominated by the CCD readout noise and the shot noise in the bright galaxy background, this technique reduced the signal-to-noise in the region by $(2)^{1/2}$. However, within the first 1.5

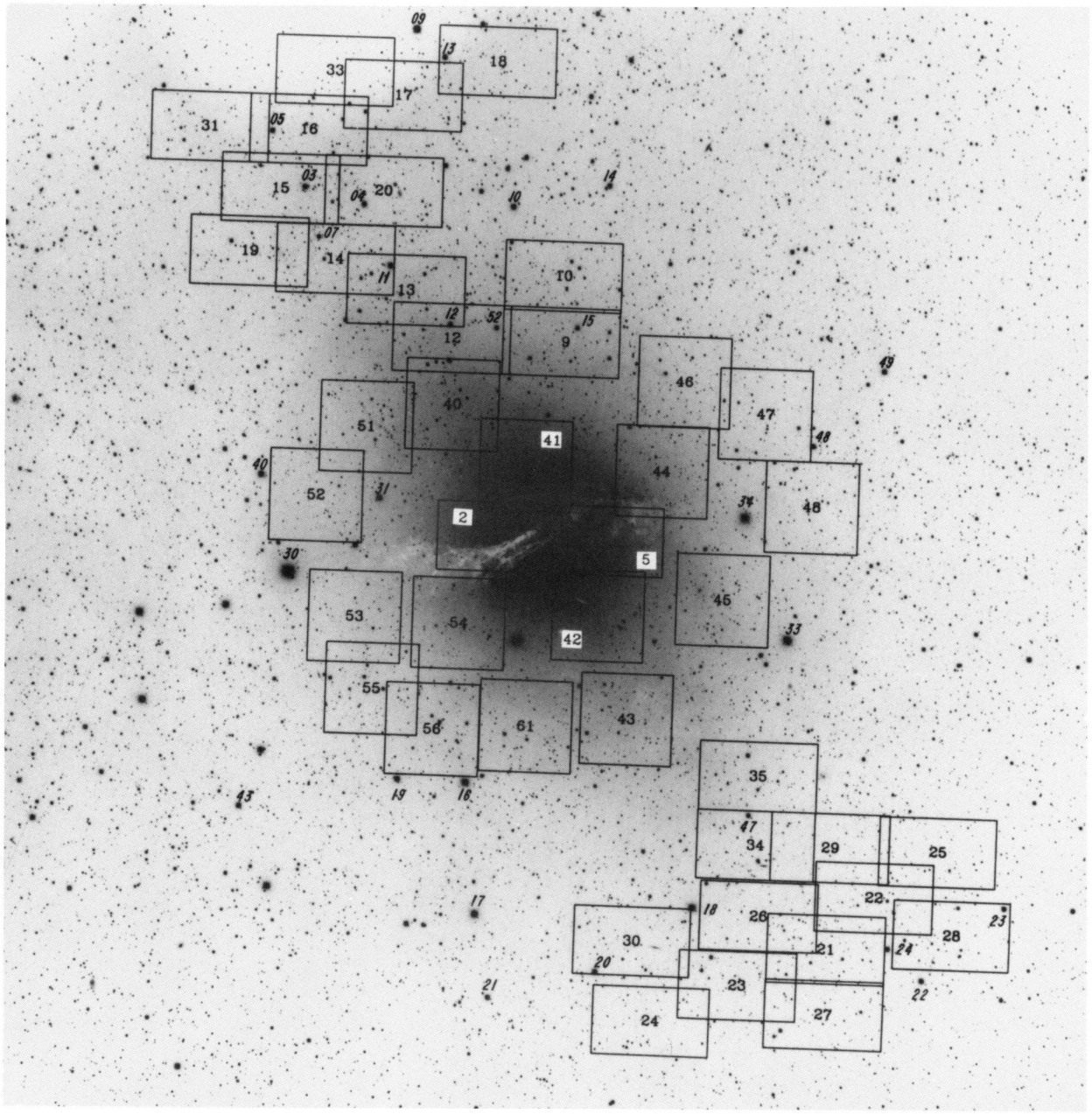

FIG. 1.—The 4 m CCD survey fields are superposed onto an image of NGC 5128 taken by J. Graham. The rectangular regions represent RCA CCD frames (5′ × 3′ or 5.1 kpc × 3.1 kpc). The square regions are TI CCD fields (4′ × 4′). The CCD frames are labeled. Also marked are the bright reference stars (slanted numbers) in Table 2 of Paper II. The centers of the most distant fields are approximately 20 kpc from the nucleus. North is at the top and east at the left.

HUI et al. (see 414, 464)

TABLE 2

JOURNAL OF OBSERVATIONS

Field	α(2000)	δ(2000)	Seeing	Air Mass[a]	UT Date
F02.....	13h25m39s66	−43°01′07″8	1″1	1.06	1985 Mar 18
F05.....	13 25 15.44	−43 01 08.7	1.0	1.03	1985 Mar 18
F09.....	13 25 26.43	−42 53 05.0	1.1	1.02	1985 Mar 19
F10.....	13 25 26.31	−42 50 24.3	1.2	1.12	1985 Mar 19
F12.....	13 25 50.63	−42 53 04.3	1.0	1.10	1985 Mar 20
F13.....	13 26 00.98	−42 51 10.8	1.4	1.05	1985 Mar 21
F14.....	13 26 16.68	−42 50 00.4	1.3	1.09	1985 Mar 21
F15.....	13 26 29.20	−42 47 11.2	1.6	1.08	1986 Apr 6
F16.....	13 26 23.19	−42 44 45.6	1.6	1.06	1986 Apr 6
F17.....	13 26 02.73	−42 43 15.8	1.4	1.25	1986 Apr 6
F18.....	13 25 42.22	−42 41 44.9	1.7	1.54	1986 Apr 6
F19.....	13 26 35.66	−42 49 46.3	1.6	1.12	1986 Apr 7
F20.....	13 26 06.46	−42 47 11.3	1.5	1.41	1986 Apr 7
F21.....	13 24 23.34	−43 17 26.1	1.1	1.12	1986 Apr 8
F22.....	13 24 13.18	−43 15 15.3	1.1	1.04	1986 Apr 8
F23.....	13 24 42.67	−43 19 02.2	1.0	1.04	1986 Apr 8
F24.....	13 25 01.74	−43 20 37.4	1.1	1.11	1986 Apr 8
F25.....	13 23 59.37	−43 13 18.9	1.3	1.33	1986 Apr 8
F26.....	13 24 38.51	−43 16 11.4	1.1	1.10	1986 Apr 9
F27.....	13 24 23.37	−43 20 06.1	1.1	1.18	1986 Apr 9
F28.....	13 23 55.65	−43 16 40.8	1.2	1.53	1986 Apr 9
F29.....	13 24 23.24	−43 13 17.8	1.1	1.03	1986 Apr 9
F30.....	13 25 06.54	−43 17 22.7	1.1	1.05	1986 Apr 9
F31.....	13 26 44.97	−42 44 44.5	1.2	1.05	1986 Apr 10
F33.....	13 26 17.77	−42 42 19.1	1.2	1.04	1986 Apr 10
F34.....	13 24 39.71	−43 13 18.1	1.2	1.19	1986 Apr 10
F35.....	13 24 39.68	−43 10 30.3	1.4	1.41	1986 Apr 10
F40.....	13 25 50.09	−42 55 48.0	1.1	1.03	1988 Apr 12
F41.....	13 25 33.51	−42 58 10.8	1.7	1.37	1988 Apr 12
F42.....	13 25 16.42	−43 04 11.9	1.0	1.06	1988 Apr 13
F43.....	13 25 09.40	−43 08 23.5	1.0	1.27	1988 Apr 14
F44.....	13 25 03.24	−42 58 14.1	1.3	1.08	1988 Apr 12
F45.....	13 24 48.86	−43 03 23.2	0.9	1.25	1988 Apr 14
F46.....	13 24 58.85	−42 54 31.9	1.2	1.63	1988 Apr 14
F47.....	13 24 40.68	−42 55 45.0	1.3	1.56	1988 Apr 13
F48.....	13 24 29.83	−42 59 28.9	1.7	1.10	1988 Apr 16
F51.....	13 26 08.81	−42 56 48.6	0.9	1.07	1988 Apr 13
F52.....	13 26 19.53	−42 59 40.6	1.1	1.11	1988 Apr 14
F53.....	13 26 10.27	−43 04 34.2	0.9	1.03	1988 Apr 14
F54.....	13 25 47.31	−43 04 42.8	1.0	1.16	1988 Apr 13
F55.....	13 26 06.03	−43 07 29.8	1.0	1.22	1988 Apr 13
F56.....	13 25 52.43	−43 09 04.8	1.5	1.31	1988 Apr 16
F61.....	13 25 31.76	−43 08 49.5	1.5	1.35	1988 Apr 16

[a] The effective air Mass during a 1 hr exposure (Stetson 1989).

mag of the PNLF, the PNs are sufficiently bright to afford this signal-to-noise loss.

In 1988 the reduction process was essentially the same. In the PSF fitting routine, we set the *fitting radius to the optimum radius* of 0.7 times the FWHM (full width at half-maximum), which is appropriate if the stellar profile is a Gaussian and the sum of the sky shot noise and the readout noise dominates the error term. Thus, our *fitting radii* varied from 2.2 to 4.1 pixels depending on the seeing conditions. The sky level was then measured in a ring between 15 and 25 pixels around each object. Again, to improve the photometry of the inner fields 41 and 42, our measurements were performed on difference pictures made by subtracting the off-band images from the on-band frames. For the remaining fields, the measurements were made directly on the on-band images.

3. PN FLUX CALIBRATIONS

We converted PN instrumental magnitudes to aperture magnitudes and then calibrated the aperture magnitudes to the [O III] λ5007 fluxes through the observations of photometric standard stars (Jacoby, Quigley, & Africano 1987), taking into account the filter transmission, the exposure time, and the atmosphere extinction (assuming $A_{5007} = 0.19$; Stone & Baldwin 1983). The monochromatic [O III] λ5007 fluxes were then converted to m_{5007} following the convention

$$m_{5007} = -2.5 \log F_{5007} - 13.74 \quad (1)$$

(Ciardullo et al. 1989a). The overall procedure was straightforward, but the following few points need some discussion.

3.1. *Aperture Corrections*

Because the PN instrumental magnitudes were derived solely from the counts within the *fitting radius*, they could not be used directly for the flux calibrations. To convert our PN instrumental magnitudes to aperture magnitudes, we chose a few bright reference stars with well-defined, unsaturated profiles in each CCD frame and derived their instrumental magnitudes in the same manner as PNs. We then measured the magnitudes of these stars through a series of concentric apertures using the DAOPHOT routine PHOT and plotted the

magnitude difference of the two adjacent apertures as a function of radius. For each CCD frame, our "aperture for total light" was defined to be the radius where the two magnitudes differed by less than ~0.005 mag (0.5%). On average, these final apertures were 3.5–4 times the FWHM of the seeing disks, or 7–8 pixels for the RCA CCD frames and 13–20 pixels for the TI CCD frames. Finally, we computed aperture corrections for our PN instrumental magnitudes by averaging the differences of the instrumental and aperture magnitudes of these reference stars.

3.2. *Interference Filters*

The selection of the filter bandpass balances the desire to eliminate both foreground and backgound light and the need to allow enough velocity coverage to account for the stars' rotation and velocity dispersion. The filter transmission should change little over the velocity range of the objects. These conditions led us to select on-band filters with ~30 Å FWHM.

Two narrow-band filters were used for the three surveys. The filter used in 1988 was well calibrated in a simulated f/2.77 beam before the observing run. However, the calibration of the filter "5016/28" used for 1985 and 1986 runs needs some discussion. The transmission of this filter was measured in nearly parallel light just before the 1985 run and immediately after the 1986 run. However, the filter transmission curve changes rapidly for any light beam faster than f/8. To understand the filter characters at the prime focus of the CTIO 4 m, we measured the filter again at KPNO in 1988 November in both a f/13 beam and a simulated f/2.77 beam. For comparison, the three measurements of the filter "5016/28" in nearly parallel beams are given in Table 3. Also listed in the last line of the table under column "1988 Nov 12" are the measured filter parameters in an f/2.77 beam. Because the central wavelength blueshifts 10 Å from an f/13 beam to an f/2.77 beam in 1988, we applied the 10 Å correction to the 1985 and 1986 filter measurements. The results are also given in the bottom line of the table. Since the bandwidth in parallel light did not change for the three measurements, we adopted the 1988 measurement of FWHM = 27 Å for all three cases.

The filter transmission curves of the three observing runs are shown in Figure 2. These curves are accurate to ~2 Å. Also shown is the velocity histogram of PNs observed in our spectroscopic program (Paper III). Clearly, the intrinsic velocity dispersion and rotation of the galaxy shifts some of the observed PNs onto the shoulder of the filter transmission function. Consequently, were we to use a constant filter transmission, such as that measured at the central wavelength, T_{λ_c}, we would underestimate the fluxes of those PNs that have [O III] λ5007 shifted off the filter center. In principle, we could correct for this effect if the velocity of every PN were individually known, but, when a nebula sits on the wing of a filter, even a 1 Å uncertainty in the filter's central wavelength produces an unacceptably large error in the correction. So, instead of correcting the PN measurements individually, we calculated a statistical correction to the PN fluxes by convolving the filter transmission curve with the PN velocity distribution and deriving an average $\bar{T}_{5007}$ for the PNs (see Jacoby et al. 1989). This correction lowered the effective transmission of the filter to $\bar{T}_{5007} = 0.947$, 0.979, and $0.987 T_{\lambda_c}$ for the 1985, 1986, and 1988 data, respectively. These values correspond to changes of 0.059, 0.023, and 0.014 mag to the computed m_{5007} magnitudes. Since the modifications are small, especially for the 1986 and 1988 data, we simply used T_{λ_c} for the calibrations.

TABLE 3

FILTER "5016/28" MEASUREMENTS

PARAMETER	DATE		
	1985 Feb 26	1986 Apr 9	1988 Nov 12
Place	Andover	CTIO	KPNO
f-ratio	f/13	f/30	f/13
Temperature	6°6 C	20° C	24° C
λ_c/FWHM(Å)	5028/25	5028/25	5024/25
λ_c/FWHM(Å)[a]	5031/25	5029/25	5024/25
λ_c/FWHM(Å)[b]	5021/27	5019/27	5014/27

[a] Normalized to an ambient temperature 24° C, assuming +1 Å shift per +5° C.

[b] In an f/2.77 beam and at a temperature of 24° C.

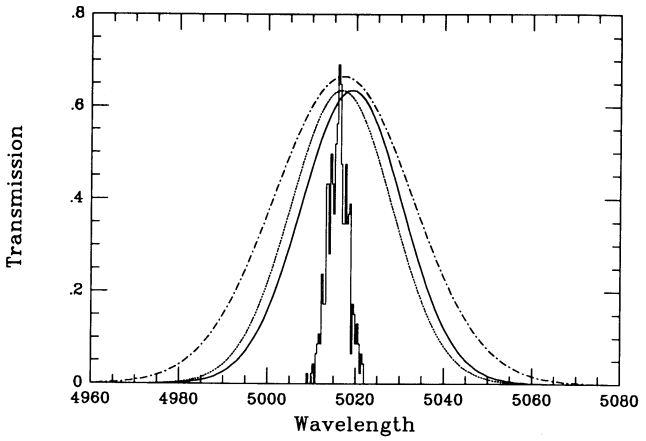

FIG. 2.—Filter transmission curves for the three surveys. The solid, dotted, and dot-dash lines are for 1985, 1986, and 1988 runs, respectively. The filter characteristics are for an f/2.77 beam and at the observing temperatures. Also presented is a PN velocity histogram with an arbitrary vertical scale.

3.3. *Photometric Accuracy*

A major uncertainty which could introduce a systematic error in the flux calibration comes from the aperture photometry. Due to the large apertures used for the absolute photometry, even a small offset in the determination of the local sky can result in a few percent error in the magnitudes of the bright reference stars or the photometric standards. However, this uncertainty can be estimated by comparing the photometry of stars in overlapping CCD frames. Out of the 43 CCD fields surveyed, we were able to identify stars in 20 regions of field overlap. From these data, the estimated error caused by the aperture photometry of both the reference and standard stars is ~1% on average, and less than ~2% in general. This is true not only for frames taken in the same year, but also holds when we compare data from different years. Because a large number of frames are involved, the error in the zero point of individual frames can be considered as a small random error when the PN samples are merged together.

The stars and PNs in the overlap regions can also give an estimate of the random errors in the PN fluxes. In Figure 3 we plot the magnitude differences against the apparent magnitude for objects with multiple measurements. Based on the data, we derived a 1 σ photometric error as a function of m_{5007} (Table 4). The photometric error is about 3% for the brightest PN ($m_{5007} = 23.6$), and increases to ~7% at 1.5 mag down the

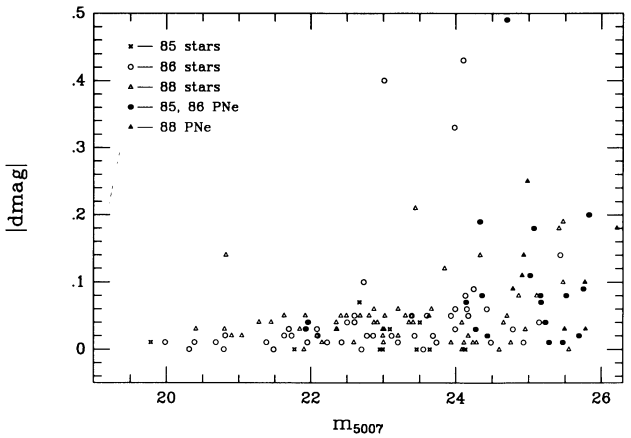

FIG. 3.—Magnitude differences of stars and PNs in the overlapping regions vs. their apparent magnitudes. The data imply that the internal photometric error is ~3% for the brightest planetary in the sample, and ~7% 1.5 mag down the PNLF.

PNLF. Additionally, the filter calibration probably gives rise to another 5% systematic error in the PN fluxes.

4. PN POSITION MEASUREMENTS

4.1. *Astrometry Solution*

We derived the PN coordinates using the Space Telescope Institute's (STScI) Guide Star Selection System (GSSS). The GSSS not only allows access to stars with cataloged positions, but also provides software to measure the positions of stars in their PDS scans of the sky survey plates (in our case, the UK SERC J southern sky survey). Our CCD frames are so small that they seldom contain stars with a listed position in the Guide Star Catalog (GSC). Consequently, in each field, we selected approximately 20 "reference stars" which are visible on the SERC Schmidt plate No. 270. We then used the GSSS program SPAM (Special Plate Analysis and Measurement) to display and measure the positions of reference stars on the archived PDS scan of plate 270. This program calculates the (x, y) centroid of designated stars and then uses the GSSS plate solution to convert (x, y) to right ascension (α) and declination (δ) in the GSC coordinate system.

In each CCD field, we converted the reference stars' (α, δ) to standard coordinates with the telescope's optical axis as the tangent point (cf. van de Kamp 1967). Using these reference stars, the transformation of (x, y) on each CCD frame to the standard coordinate system was then derived by a multiple linear regression method. Only linear terms, which account for the shift, scale, and rotation of the two coordinate systems, proved to be necessary. Because of the low galactic latitude of NGC 5128, the presence of a large number of foreground stars facilitated the process. The average root-mean-square residuals of the transformations were 0".17, 0".13, and 0".11 in each coordinate for the 1985, 1986, and 1988 data, repectively. Finally the PNs' CCD positions were converted to equatorial coordinates using the derived solutions. Although this procedure does not account for the proper motion of the reference stars between the epochs of the SERC plates and the CCD frames, our experience shows that this is not a major source of errors.

Fields 2 and 5 project onto NGC 5128's bright central region, where the high-density background allows fewer reference stars to be located on the Schmidt plate and the steep background gradient causes larger positional uncertainties. As a result, only about 10 reference stars were measured in these fields, and no satisfactory astrometric solution could be derived from these stars alone. We therefore used PNs in the regions overlapping the 1988 data to better constrain the astrometry. There were nine PNs appearing on both fields 2 and 41. Their equatorial coordinates derived in field 41 were used together with those of 10 reference stars to derive the astrometric solution for field 2. Similarly, the transformation for field 5 was derived from 12 reference stars and 18 PNs which are on both fields 5 and 44 or 5 and 42. The rms of the solution for both fields is about 0".16 in each coordinate, identical to those of the halo fields.

TABLE 4

PHOTOMETRIC ERROR VS. m_{5007}

m_{5007}	Numbers of Objects	σ(mag)
21.5.....	18	0.017 ± 0.004
22.3.....	11	0.023 ± 0.005
22.8.....	18	0.032 ± 0.006
23.3.....	16	0.038 ± 0.012
23.7.....	8	0.026 ± 0.009
24.0.....	7	0.039 ± 0.016
24.3.....	15	0.050 ± 0.015
24.7.....	15	0.055 ± 0.018
25.1.....	8	0.068 ± 0.020
25.5.....	8	0.081 ± 0.028
25.8.....	6	0.092 ± 0.033

4.2. *Astrometry Accuracy*

The internal errors were checked by comparing the star positions measured in the overlapping areas of 29 pairs of CCD fields. Based on 107 stars in the 1985 and 1986 samples and 62 stars of the 1988 data, we estimate that the 1 σ random error in each coordinate is 0".09.

To estimate the external accuracy of the coordinates, we excluded bright reference stars from the solutions and then compared their derived positions with their GSSS measured positions. The resulting mean difference and rms dispersion are 0".02 and 0".09 in each coordinate for 18 stars in the 1985 and 1986 samples. For 30 stars in the 1988 data, the corresponding values are −0".02 and 0".11. Hence, no systematic errors are present, and the 1 σ random error of reference stars with respect to the Guide Star Catalog is 0".1.

These comparisons indicate that the positions of reference stars and PNs are accurate to 0".2 in each coordinate with respect to the Guide Star Catalog.

5. NGC 5128 PNS

The PN spatial distribution is shown in Figure 4, where the ellipses represent the approximate isophotes of the galaxy at a step size of $1r_e$. Because the PN catalog is very long, it will be published in the *Astrophysical Journal Supplement* (Paper II). Also appearing there is a set of 32 stars selected from the Guide Star Catalog, and a collection of 80 secondary reference stars measured on Schmidt plate No. 270 using the GSSS software. These stars can be used for astrometric references in future observations with instruments such as multifiber spectrographs.

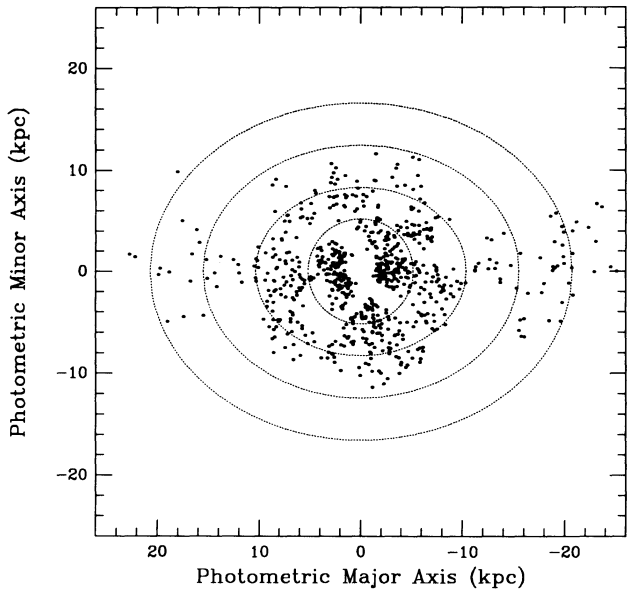

FIG. 4.—Spatial distribution of all 785 PNs. The ellipses are the approximate isophotes of NGC 5128, and are shown at 1, 2, 3, and 4 effective radii.

6. NGC 5128's PNLF AND ITS DISTANCE

6.1. *Planetary Nebula Luminosity Function*

In a simple model, a PN's nebular shell is described as a uniformly expanding sphere of ionized gas (Henize & Westerlund 1963). If the central star evolves slower than shell expansion, then the decline of the [O III] λ5007 line brightness is mostly due to the expansion. The corresponding PNLF is

$$\Phi(m) \propto e^{0.307m}\,, \tag{2}$$

where $\Phi(m)dm$ is the number of PNs between magnitudes m and $m + dm$. Function (2) fits the PNLF of the Magellanic Clouds (Jacoby 1980) and M31 (Ciardullo et al. 1989a) extremely well, except for the brightest 0.8 mag, where a sharp falloff is observed. To accommodate the observations, Ciardullo et al. (1989a) introduced an empirical function

$$\Phi(m) \propto e^{0.307m}[1 - e^{3(m^* - m)}] \tag{3}$$

where the parameter m^* defines the PNLF cutoff. This cutoff, if it is universal, is a standard candle. If M31 is at a distance of 710 kpc (Welch et al. 1986) and has a differential extinction $E(B-V) = 0.11$, then an absolute magnitude of $M^* = -4.48$ is implied by M31's PNLF. This value serves as the zero point of the PNLF distance scale. Any observation of m^* gives an estimate of the distance modulus of the galaxy, $\mu = m^* - M^*$.

6.2. *Sample Completeness*

Only those PNs in the brightest 2–3 mag of PNLF were detected in our surveys. Fainter PNs are lost in the galaxy and sky background noise. But long before this, at about 1.5 mag magnitudes below the PNLF cutoff, incompleteness becomes important. In the galaxy halo, sky background dominates the light, and the *limiting magnitudes* (where sample incompleteness becomes significant) of CCD frames taken in comparable seeing are similar. However, in the galaxy's inner regions, the steep gradient in background surface brightness makes our PN sample more and more incomplete toward the nucleus. Because at one effective radius ($r_e \approx 5'$), NGC 5128's V-band surface brightness of $\sim$22 mag per square arcsec (D79) is comparable to the CTIO sky brightness, the effect of the bright galaxy background becomes important within this area.

We studied the limiting magnitude as a function of isophotal radius by comparing the PN distribution with that of the light sampled in our CCD frames. NGC 5128's isophotes change in ellipticity, from $b/a = 0.93$ at $r = 2'.6$ to $b/a = 0.74$ at $r = 9'.0$ (D79). Accordingly, we calculated the isophotal radius of individual nebulae by linearly interpolating between the ellipticities given above and taking a constant value of $b/a = 0.74$ beyond $r = 9'.0$. We then performed a similar calculation for the galaxy's luminosity distribution, using the same ellipticity law and the surface brightness profile

$$\sigma_V = 8.32\left[\left(\frac{r}{r_e}\right)^{1/4} - 1\right] + 22.00\,, \tag{4}$$

where $r_e = 305''$ (D79). The distribution of both the PNs and the light is shown in Figure 5, with the heavily obscured fields 2 and 5 excluded from the analysis. The figure indicates that PNs follow the luminosity distribution well for $r \gtrsim 6'$, confirming that the limiting magnitude in the galaxy's halo is approximately constant. The deficiency of PNs at smaller radii is partly due to the bright galaxy light which causes incompleteness to set in at progressively brighter magnitudes, and partly a color effect (§ 8).

One conventional method of determining the limiting magnitude of a CCD frame is to add artificial stars of various brightness, and try to recover them using the same process used to identify PNs. The rate of successful recovery as a function of magnitude tells when the sample incompleteness becomes important and allows the limiting magnitude to be determined. However, because the limiting magnitudes of our CCD frames change with both the galaxy background and the seeing, this method is impractical. Instead, we restrict our sample of PNs to only those objects with $r > 6'$ and compare their PNLF to a properly scaled and shifted empirical law. This is done in Figure 6, which plots the dereddened PN magnitudes, using an assumed differential extinction of $E(B-V) = 0.1$ (van den Bergh 1976) and a Seaton (1979) reddening law. From the figure, the limiting magnitude of our PN sample is $m_l \approx 24.8$.

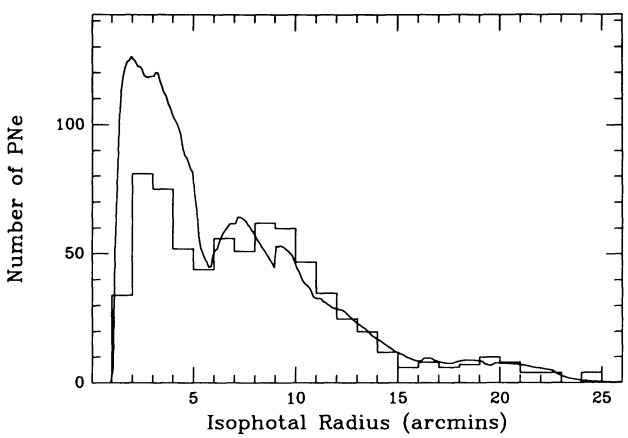

FIG. 5.—Histogram showing the distribution of isophotal radii for all PN candidates, excluding those objects in the heavily obscured fields 2 and 5. The solid line displays the corresponding amount of V luminosity surveyed. A comparison shows that beyond 6′, the PNs follow the galaxy's luminosity, and suggests that the limiting magnitude in this region is constant.

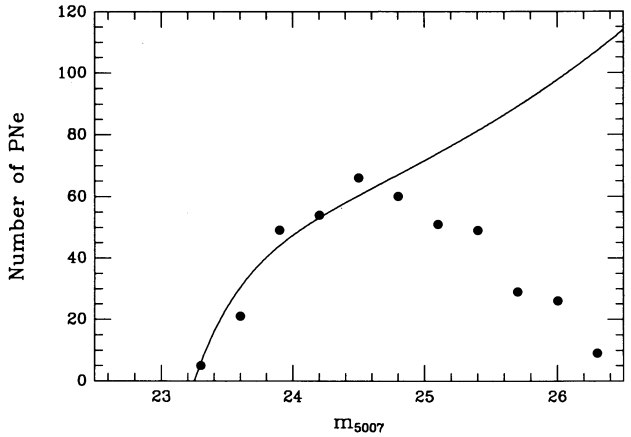

FIG. 6.—NGC 5128's planetary nebula luminosity function is compared with the empirical PNLF of equation (3). The PNs are binned into 0.3 mag intervals. The m_{5007} magnitudes are corrected for a foreground extinction of $E(B-V) = 0.1$.

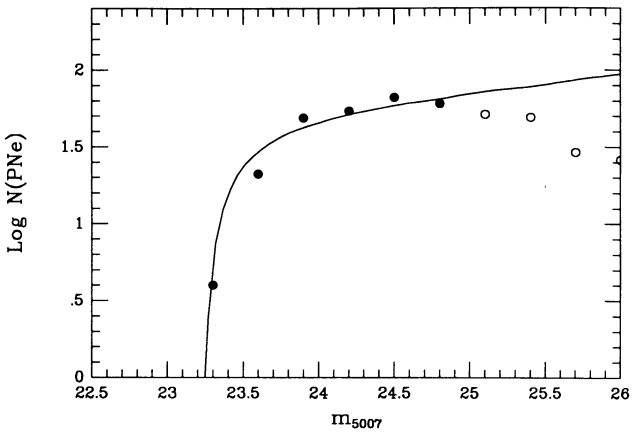

FIG. 8.—Observed PNLF of NGC 5128 derived from a complete sample of halo objects. The data have been binned into 0.3 mag intervals. The solid line shows the empirical PNLF convolved with the mean photometric error vs. magnitude relation and translated to the most likely distance modulus. Open circles show PNs below the completeness limit, which were excluded from the fit.

To check this result, we used the 1 σ error in instrumental magnitudes given by DAOPHOT to estimate the PN signal-to-noise ratio (SNR = $1.086/\sigma_{mag}$) within the fitting radius. The result is shown in Figure 7. It is clear that a minimum SNR of 5 is needed for a PN to be identified, and almost every nebula above a limiting magnitude 24.8 has a SNR higher than 10. In their study of the M31 novae, Ciardullo et al. (1987) used DAOPHOT to add artificial stars into their on-band image and attempted to recover them through a blinking procedure similar to our PN identification process. They found that the completeness was close to 100% when the SNR was greater than 9, but decreased to 0 when the SNR was less than 4. This is in excellent agreement with our results, and thus we conclude that $m_l = 24.8$ is a realistic estimate of the limiting magnitude of the halo frames.

6.3. *The Distance to NGC 5128*

If we adopt a limiting magnitude $m_l = 24.8$, we can form a complete sample of 224 PNs with isophotal radius $r > 6'$. We call this set of data sample A. To derive the distance to NGC 5128, the empirical PNLF equation (3) is numerically convolved with the PN photometric errors of Table 4 and compared to the observed PNLF using the method of maximum likelihood (Ciardullo et al. 1989a). This produces a most likely true distance modulus of $(m - M)_0 = 27.73^{+0.03}_{-0.05}$. The best estimate of the luminosity specific PN density is $\beta_{2.5} = 99 \pm 10 \times 10^{-9}\ L_\odot^{-1}$. This number is scaled to 2.5 mag below the bright cutoff, but normalized in the B band rather than in bolometric light due to the lack of proper multicolor infrared photometry. Figure 8 is a logarithmic plot of NGC 5128's PNLF along with the best-fit empirical function (3). In deriving the distance, we have excluded the "brightest" nebula PN 5601, which happens to fall on the bleeding tail of a bright star in the CCD image and thus has its photometry affected by these bright columns.

From the probability contours of the solution (light curves, Fig. 9), the 1 σ error in NGC 5128's distance modulus is estimated to be $+0.03/-0.05$. However, several other uncertainties also affect the derived distance, including the errors in

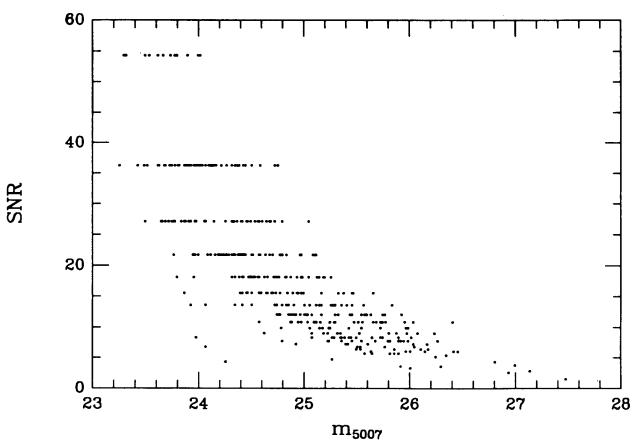

FIG. 7.—Estimated signal-to-noise vs. magnitude. Above $m_l = 24.8$, SNRs are larger than 10 for almost all nebulae; no objects were detected below a SNR of 5.

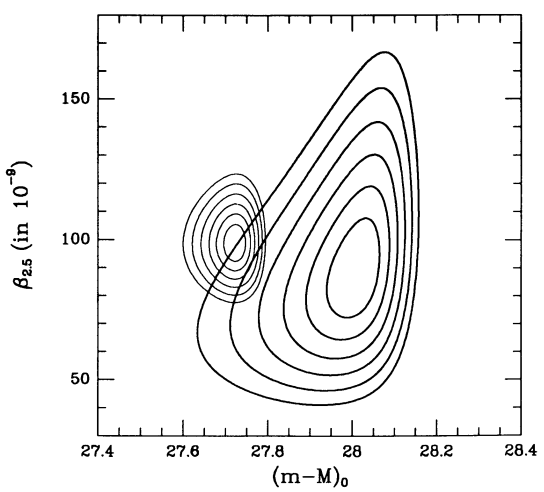

FIG. 9.—Confidence level contours of the maximum likelihood solution for both sample A (light curves) and the 1985 and 1986 halo samples (heavy curves). The abscissa is the dereddened distance modulus, and the ordinate is the B-luminosity specific PN density. The contours are shown at 0.5 σ intervals.

the adopted M31 distance (0.1 mag), the PNLF model (0.05 mag) (Jacoby et al. 1990), and the uncertainty in the filter calibration (0.05 mag). Assuming these errors are uncorrelated, the total uncertainty in the distance NGC 5128 is 0.14 mag, or 7%. Thus, the most likely distance modulus to the galaxy is $(m - M)_0 = 27.73 \pm 0.14$, which is corresponding to a distance of 3.5 ± 0.2 Mpc.

To facilitate comparison of luminosity specific PN density with other galaxies, we can assume that the bolometric correction for NGC 5128 is the same as NGC 4382, a giant elliptical in Virgo with a similar $(B-V)_0$ color. Thus, if BC $= -0.67$, then $\alpha_{2.5} = 50 \pm 5 \times 10^{-9}\ L_{\odot}^{-1}$ in bolometric luminosity. This number is not particularly sensitive to the choice of the bolometric correction because the range of corrections for giant elliptical galaxies is relatively small (Ciardullo et al. 1989b; Jacoby et al. 1990a). We can also convert $\alpha_{2.5}$ to a PN formation rate by assuming that during a typical lifetime of 25,000 years, a PN's luminosity decreases by ~ 8 mag following equation (3) (Jacoby 1980; Ciardullo et al. 1989a). The resulting PN formation rate is $20 \times 10^{-12}\ \mathrm{yr}^{-1}\ L_{\odot}^{-1}$.

In the above discussions, we assumed that the NGC 5128 PNLF follows the empirical form of equation (3). However, a maximum likelihood analysis by itself does not prove this a priori assumption is correct. In order to statistically test NGC 5128's PNLF against the empirical function, we performed a one-sample, two-sided Kolmogorov-Smirnov test. Given the best estimate of $\mu = 27.73$, the largest difference of the two cumulative distributions is $D_{\max} = 0.067$. With the sample size of 224, the corresponding significance level is 27%. In other words, the probability of obtaining a $D_{\max} = 0.067$ or larger is 27% if the empirical form is the true representation of the NGC 5128's PNLF. Therefore, the KS test cannot distinguish NGC 5128's PNLF from the empirical function.

6.4. *Comparison with Other Methods of Distance Measurement*

An elliptical galaxy such as NGC 5128 has remarkably few observational quantities that can be used to reliably estimate its distance. Based on the sizes of H II regions and on galaxy luminosity classifications, Sandage & Tammann (1975) estimated the distance to two spirals in the NGC 5128 Group to be 7.9 Mpc, but de Vaucouleurs (1979) derived a much smaller value of 3.3 ± 0.1 Mpc for the galaxy from its redshift and its group membership. By comparing NGC 5128's globular cluster luminosity function with that of the Galaxy and M31, Harris, Harris, & Hesser (1986) derived a galaxy distance of 3.2 Mpc, but since this estimate was based only on the brightest globular clusters and the Gaussian peak of the luminosity function was not reached, the value has a considerable uncertainty. Another estimate of NGC 5128's distance comes from Frogel et al. (1987), who compared the H-band maximum brightness of the Type Ia SN 1986g to that of SN 1984a in the Virgo galaxy NGC 4419. Their relative distance modulus of 3.37, when combined with the PNLF distance modulus of Virgo (30.84; Jacoby et al. 1990a), yields $(m - M)_0 = 27.47 \pm 0.33$, or 3.1 ± 0.5 Mpc for the distance to NGC 5128. Here, the formal error includes the scatter in the peak brightness of Type Ia supernovae and the error in the PNLF distance to Virgo, but does not include an additional uncertainty arising from the fact that the light curve of SN 1986g is significantly different from that of SN 1984a.

Perhaps the best estimate of NGC 5128's distance is derived from the surface brightness fluctuation (SBF) technique. In their application of the method, Tonry & Schechter (1990) measured the galaxy's mean fluctuation magnitude and color to be $\bar{m}_I = 26.08 \pm 0.06$ and $(V-I) = 1.07$. Using these values and a revised calibration $\bar{M}_I = -4.84 + 3.0(V-I)$ (Tonry 1991), the distance to NGC 5128 becomes $(m - M)_0 = 27.71 \pm 0.10$, or 3.5 ± 0.2 Mpc. The error includes the 1 σ uncertainty in the measurement of $\bar{m}_I$ and an 0.08 mag error in the calibration of $\bar{M}_I$. This distance is remarkably consistent with that of the PNLF.

In conclusion, the most recent measurements consistently put NGC 5128's distance in the range of 3–3.5 Mpc. Based on the merits of each method, we believe the PNLF and SBF distances bear higher weights. The most likely distance to the galaxy is 3.5 ± 0.2 Mpc.

7. A TEST OF THE EFFECTS OF METALLICITY ON THE PNLF DISTANCE

Cosmic variations in the PNLF will be minimized if the nebulae are observed in the similar populations found in elliptical galaxies and in the bulges of spiral galaxies. However, even with this limitation, the target galaxies are not uniform in their stellar population. It is well known that the broad-band colors of ellipticals are correlated with their absolute luminosities. This color-magnitude relation is further complemented by spectroscopic metallicity indicators, such as Mg_2, which suggest that metallicity is the key parameter in the relation. Moreover, it is commonly believed that the same metallicity dependence is also responsible for the observed color gradients within individual elliptical galaxies (Kormendy & Djorgovski 1989 and references therein). Generally, [Fe/H] is thought to decrease by 0.2 dex from the center to one effective radius, and observations of the Mg_2 gradient in three elliptical galaxies of the Coma Cluster have shown that the metal abundance in these galaxies probably drops by a factor of 3 or 4 between the nuclear region and $3r_e$ (Baum, Thomsen, & Margon 1986; Thomsen & Baum 1987, 1988).

Metallicity affects the [O III] λ5007 PNLF in two ways. On the one hand, the [O III] λ5007 emissivity depends on the metallicity of the nebula, especially the oxygen abundance. However, this dependence is relatively weak because as a principal coolant, the [O III] λ5007 line acts as a thermostat. As metallicity decreases, the electron temperature rises, and the emission-line strength is enhanced to maintain the balance between heating and cooling. As a result, the [O III] λ5007 brightness changes as the square root of the oxygen abundance (Jacoby 1989). On the other hand, metallicity affects both the mass loss on the asymptotic giant branch and the time scales of stellar evolution. Consequently, the core mass of the central stars and thus the [O III] λ5007 luminosity depend on metallicity.

Because PNs are detected from the inner region of NGC 5128 to its outer halo, the metallicity effect may be examined by subdividing the PN sample by spatial distribution. We have done this using the 1988 data and the combined 1985 and 1986 halo data. Table 5 gives the results, where the columns are the PN isophotal radius range, the average PN isophotal radius, the apparent galactic brightness m_B sampled in the CCD frames, the number of observed PNs brighter than $m_l = 24.5$, the derived distance modulus, and the B-band luminosity specific PN density, $\beta_{2.5}$. The PNLFs for each subsample are shown in Figure 10 along with the best-fitting empirical function. Notice that a brighter limiting magnitude of 24.5 is used in each calculation in order to accommodate the inner region

TABLE 5

NGC 5128 DISTANCES DERIVED FROM SUBSAMPLES

PN Sample	$\bar{r}$	m_B	N	$(m-M)_0$	$\beta_{2.5}$
88 (1′–3′)[a]	2.3	9.86	61	27.72	82.7
88 (3′–6′)	4.3	9.52	67	27.72	66.0
88 (6′–9′)	7.4	10.09	64	27.76	108.0
88 (9′–16′)[b]	11.0	10.34	54	27.67	111.5
1985 and 1986 halo	15.2	10.20	43	28.01	89.0

[a] In field 41, the area inside of isophotal radius of 1.5 is partly obscured by the dust lane and is excluded.

[b] Without PN 5601; see § 6.3.

samples (see Fig. 10). However, samples in the halo go deeper than those in the inner envelope. In particular, sample 88 (9′–16′) follows PNLF of equation (3) down to 2 mag below the bright-end cutoff.

It is apparent that the 1985 and 1986 halo data give a larger distance modulus than the value of $27.73^{+0.03}_{-0.05}$ derived using sample A, in which the 1988 data dominate. The difference is ~ 0.28 mag and accounts for the discrepancy between the value derived in this paper and that presented by Jacoby, Ciardullo, & Ford (1988). The probability contours of the maximum likelihood solution are plotted in Figure 9 for both samples. The figure shows that the solution of sample A is much better constrained than that of the 1985 and 1986 halo sample. It also shows that the difference in $(m-M)_0$ is statistically significant. This large margin is due to the fact that over 10 PNs in sample A are brighter than the brightest PN observed in the 1985 and 1986 halo data. By checking the spectra of the brightest few PNs observed in 1988, we have confirmed that the Hβ line is not present and the FWHM of the [O III] λ5007 lines is unresolved. Therefore, our sample is not contaminated by low-excitation H II regions nor are the optical doubles discussed by Jacoby et al. (1990a) important.

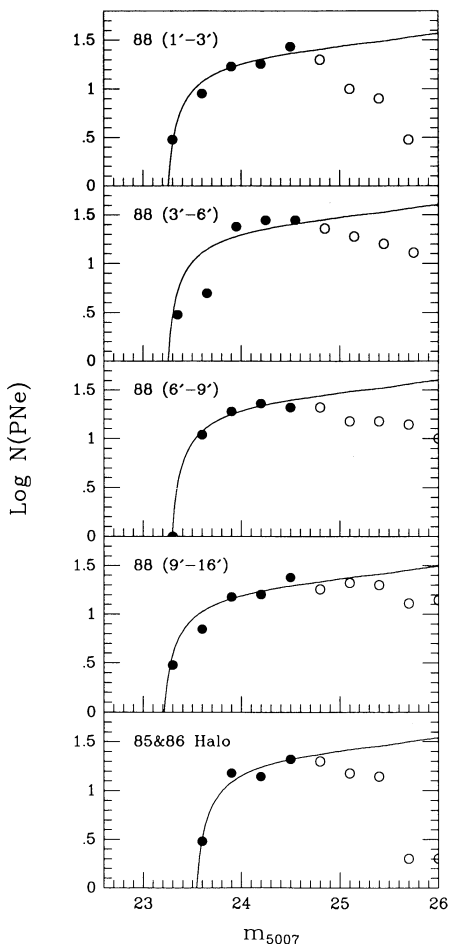

FIG. 10.—Observed PNLFs of NGC 5128 derived from samples of PNs with different isophotal radii. Once again, the data have been binned into 0.3 mag intervals. The solid lines show the empirical PNLF of eq. (3), convolved with the mean photometric error vs. magnitude relation and translated to the most likely distance modulus of each sample. PNs below the completeness limit (*open circles*) were not included in the fit.

However, both Table 5 and Figure 10 suggest that the distance measurements among the 1988 data are highly consistent. The average distance modulus of the four samples is 27.72 ± 0.02, identical to the values $27.73^{+0.03}_{-0.05}$ of sample A. Moreover, the small scatter in $(m-M)_0$ is completely consistent with that expected from normal statistical fluctuations. The lack of any systematic trend implies that the PNLF cutoff is insensitive to any possible population variation between 2 and 16 kpc. Although no detailed multicolor surface photometry exists for NGC 5128, the spatial variation of the luminosity specific PN density suggests that the galaxy becomes bluer with increasing radius (see § 8).

There are three possibilities for the discrepancy between the 1988 PNLF and that measured in 1985 and 1986. First and probably most likely, the cause of the discrepancy resides in the accuracy of the photometric calibration for the 1985 and 1986 data. Given the indirect filter calibration for the first two runs (see § 3.2), we suspect that the filter transmission curves are not known precisely. Unfortunately, there are no common PNs between the two samples available for the checking. Another possibility is that it is a real population effect. However, as the next section will show, the luminosity specific PN density is very sensitive to color gradients, and the fact that this quantity varies little over the radius range of 7–20 kpc argues against an abrupt change in the galaxy's stellar population. Finally, the difference may be entirely due to small number statistics. However, a Monte Carlo simulation shows that the probability for such a situation is less than 1%. Further surface photometry and halo PN observations may help decide which combination of these factors is responsible for the change in distance modulus in the halo.

8. LUMINOSITY-SPECIFIC PN DENSITY

Table 5 suggests that in NGC 5128, the number of PNs per unit galaxy luminosity increases with radius. This can be seen graphically in Figure 11. The solid points in the figure show the ratio between the number of PNs with $m < 24.5$ and the underlying galaxy luminosity; the open circles give the computed values of the B-band luminosity specific PN density $\beta_{2.5}$ normalized to this same limiting magnitude. Once again, the central two fields 2 and 5 are not included in the calculation. Also excluded is the area inside of isophotal radius of 1.5 in field 41, due to partial obstruction by the dust lane.

The data show that the PN/L ratio increases with radius inside 7′, then levels off between 7′ to 20′. Since only complete samples of PNs were used in deriving $\beta_{2.5}$, the consistency between the two data sets suggests that the effect is unlikely caused by sample incompleteness. If, like most elliptical galaxies, NGC 5128 becomes bluer with increasing radius, then

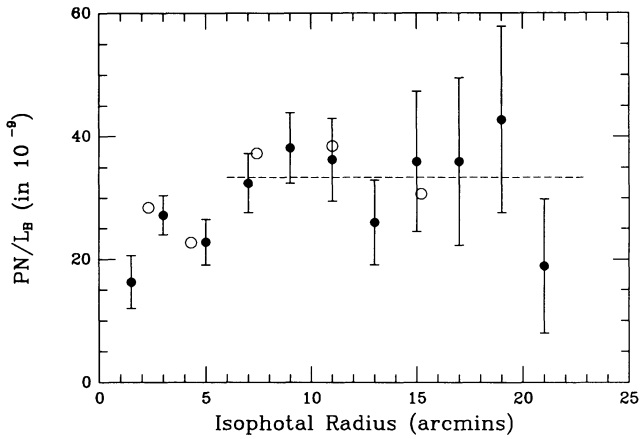

FIG. 11.—Solid points show the number of PNs brighter than $m_I = 24.5$ normalized to the galaxy B-luminosity at different isophotal radii. The open circles are values of the B-luminosity-specific PN density ($\beta_{2.5}$), normalized to the same magnitude limit. The errors bars reflect the Poisson noise in the PN number counts only. The data show that the PN/L ratio is approximately constant outside 7′, but decreases significantly within this radius.

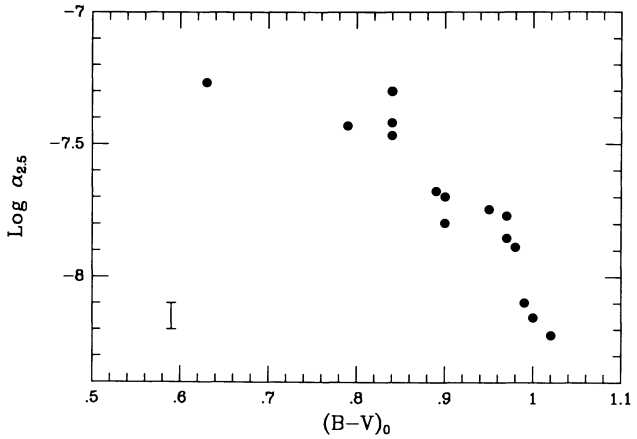

FIG. 12.—Luminosity specific PN density ($\alpha_{2.5}$) as a function of the $(B-V)_0$ color of galaxies. A typical 1 σ error bar from the maximum likelihood fits is shown in the lower left corner. The data suggest that redder stellar populations produce fewer PNs (per unit luminosity) than bluer systems. This behavior is mimicked in NGC 5128.

the data may imply that the PN/L ratio is larger for bluer stellar populations.

A similar phenomenon is also seen among other galaxies. Table 6 lists the derived values of the bolometric luminosity specific PN density ($\alpha_{2.5}$) for other galaxies. These data are plotted against galaxy $(B-V)_0$ color in Figure 12. As first noticed by Peimbert (1990), $\alpha_{2.5}$ is a strong function of color: it decreases by a factor of 7 from the value of ~ 50 seen in the dwarf elliptical NGC 205 to the typical value of ~ 7 observed in the giant elliptical galaxies of the Virgo Cluster. Given that the overall error, including those of the maximum likelihood solution and the luminosity normalization, is typically $\sim 30\%$ in an individual measurement of $\alpha_{2.5}$ (Ciardullo et al. 1991), this systematic trend is most likely real. Furthermore, the fact that populations with similar colors (such as that of M31's bulge, M104, and NGC 4374) have similar luminosity specific PN densities, despite their drastically different distances, argues strongly that the $\alpha_{2.5}$-color relation is a not an artifact of the reductions or observational limits, but is an intrinsic property of stellar populations. The gradient in the PN/L ratio seen in NGC 5128 supports this conclusion.

9. SUMMARY

We have presented the results of a PN survey of NGC 5128 and have demonstrated that large numbers of PNs can be found out to a galactic radius of four effective radii. Photometry of these PNs reveals that the first 1.5 mag of NGC 5128's PN luminosity function is statistically identical to that measured in M31 central bulge. If we adopt a foreground differential extinction of $E(B-V) = 0.1$, then the implied distance to NGC 5128 is 3.5 ± 0.2 Mpc. This number is in perfect agreement with that determined from the surface brightness fluctuation method (Tonry & Schechter 1990 and Tonry 1991).

We have used our large sample of PNs to look for changes in the PNLF with galactic radius. No population effect on the bright cutoff of PNLF is observed in the isophotal radius range between 2 and 16 kpc. Outside of 7 kpc, the luminosity specific PN density also appears to be invariant, as the PN spatial distribution follows the luminosity profile of the galaxy. Inside of 7 kpc, however, the value of ($\alpha_{2.5}$) seems to decrease, in a manner reminiscent of the $\alpha_{2.5}$-color relation derived from other galaxies. This decrease provides further evidence that the

TABLE 6

LUMINOSITY SPECIFIC PN DENSITIES

NGC	$(B-V)_0$	$\alpha_{2.5} \times 10^9$	Reference
205.....	0.63	54	Ciardullo et al. 1989a, Burstein et al. 1987
224.....	0.84	34	Ciardullo et al. 1989a, Burstein et al. 1987
221.....	0.97	14	Ciardullo et al. 1989a, Kent 1987
3031.....	0.90	16	Jacoby et al. 1989, Brandt et al 1972
3377.....	0.79	37	Ciardullo et al. 1989b
3379.....	0.89	21	Ciardullo et al. 1989b
3384.....	0.84	38	Ciardullo et al. 1989b
4374.....	0.97	17	Jacoby et al. 1990a
4382.....	0.90	20	Jacoby et al. 1990a
4406.....	0.98	13	Jacoby et al. 1990a
4472.....	1.00	7	Jacoby et al. 1990a
4486.....	0.99	8	Jacoby et al. 1990a
4649.....	1.02	6	Jacoby et al. 1990a
4594.....	0.95	22	Ford et al. 1993
5128.....	0.84	50	This paper

variation in $\alpha_{2.5}$ discussed by Peimbert (1990) and Ciardullo et al. (1991) is real and not an artifact of incompleteness or systematic errors in PNLF distances.

This paper is based on part of a Ph.D thesis by Xiaohui Hui at Boston University. We are indebted to Don Neill for his work at the earlier stage of the data reduction, and to the staff of the Guide Star Catalog Project at the Space Telescope Science Institute for their assistance. This work was supported in part by NASA grant NAG 5-1630. R. C. acknowledges the support of NASA grant NAGW-3159 and NSF grant AS 792-57833.

REFERENCES

Baum, W. A., Thomsen, B., & Margon, B. L. 1986, ApJ, 301, 83
Brandt, J. C., Kalinowski, J. K., & Roosen, R. G. 1972, ApJS, 24, 421
Burstein, D., Davies, R. L., Dressler, A., Faber, S. M., Stone, R. P. S., Lynden-Bell, D., Terlevich, R. J., & Wegner, G. 1987, ApJS, 64, 601
Ciardullo, R., Ford, H. C., Neill, J. D., Jacoby, G. H., & Shafter, A. W. 1987, ApJ, 318, 520
Ciardullo, R., Ford, H. C., Williams, R. E., Tamblyn, P., & Jacoby, G. H. 1990, AJ, 99, 1079
Ciardullo, R., Jacoby, G. H., & Ford, H. C. 1989b, ApJ, 344, 715
Ciardullo, R., Jacoby, G. H., Ford, H. C., & Neill, J. D. 1989a, ApJ, 339, 53
Ciardullo, R., Jacoby, G. H., & Harris, W. E. 1991, ApJ, 383, 487
de Vaucouleurs, G. 1979, AJ, 84, 1270
Dufour, R. J., van den Bergh, S., Harvel, C. A., Martins, D. H., Schiffer, F. H. III, Talbot, R. J. Jr., Talent, D. L., & Wells., D. N. 1979, AJ, 84, 284 (D79)
Ford, H. C., Hui, X., Ciardullo, R., Jacoby, G. H., & Freeman, K. C. 1993, ApJ, submitted
Ford, H. C., & Jenner, D. C. 1978, BAAS, 10, 665
Frogel, J. A., Gregory, B., Kawara, K., Lavey, D., Phillips, M. M., Terndrup, D., Urba, F., & Whitford, A. E. 1987, ApJ, 315, L129
Graham, J. A. 1979, ApJ, 232, 60
Harris, H. C., Harris, G. L. H., & Hesser, J. E. 1986, in IAU Symp. 126, The Harlow Shapley Symposium on Globular Cluster Systems in Galaxies, ed. J. E. Grindlay & A. G. D. Philip (Dordrecht: Reidel), 205
Henize, K. G., & Westerlund, B. E. 1963, ApJ, 137, 747
Hui, X., Ford, H. C., Ciardullo, R., & Jacoby, G. H. 1993a, ApJS, in press, (Paper II)
Hui, X., Ford, H. C., Freeman, K. C., & Dopita, M. A. 1993b, ApJ, submitted (Paper III)
Jacoby, G. H. 1980, ApJS, 42, 1
———.1989, ApJ, 339, 39
Jacoby, G. H., Branch, D., Ciardullo, R., Davies, R. L., Harris, W. E., Pierce, M. J., Pritchet, C. J., Tonry, J. L., & Welch, D. L. 1992, PASP, 104, 599
Jacoby, G. H., Ciardullo, R., & Ford, H. C. 1988 in The Extragalactic Distance Scale, ASP Conf. Series No. 4, ed. S. van den Bergh & C. J. Pritchet (Provo: Brigham Young Univ. Press), 42
———. 1990a, ApJ, 356, 332
Jacoby, G. H., Ciardullo, R., Ford, H. C., & Booth, J. 1989, ApJ, 344, 704
Jacoby, G. H., & Lesser, M. P. 1981, AJ, 86, 185
Jacoby, G. H., Quigley, R. J., & Africano, J. L. 1987, PASP, 99, 672
Jacoby, G. H., Walker, A. R., & Ciardullo, R. 1990b, ApJ, 365, 471
Kent, S. M. 1987, AJ, 94, 306
Kormendy, J., & Djorgovski, S. 1989, ARA&A, 27, 235
Oke, J. B. 1974, ApJS, 27, 21
Peimbert, M. 1990, Rep. Prog. Phys., 53, 1559
Sandage, A. R., & Tammann, G. A. 1975, ApJ, 196, 313
Seaton, M. J. 1979, MNRAS, 187, 73P
Stetson, P. B. 1987, PASP, 99, 191
———. 1989, Highlights Astron. 8, 635
Stone, R. P. S. 1977, ApJ, 218, 767
Stone, R. P. S., & Baldwin, J. A. 1983, MNRAS, 204, 347
Thomsen, B., & Baum, W. A. 1987, ApJ, 315, 460
———. 1989, ApJ, 347, 214
Tonry, J. L. 1991, ApJ, 373, L1
Tonry, J. L., & Schechter, P. L. 1990, AJ, 100, 1794
Welch, D. L., McAlary, C. W., McLaren, R. A., & Madore, B. F. 1986, ApJ, 305, 583
van de Kamp, P. 1967, in Principles of Astrometry, with Special Emphasis on Long-Focus Photographic Astrometry (San Francisco: W. H. Freeman), 73
van den Bergh, S. 1976, ApJ, 208, 673